HUNGARIAN UNIVERSITY OF AGRICULTURE AND LIFE SCIENCES

Tribological applicability of polymer composites in farm-machines

PhD Thesis

by

Hasan Muhandes

Gödöllő
2021

Doctoral school

Denomination: Doctoral School of Mechanical Engineering

Science: Mechanical Engineering

Leader: Prof. Dr. István Farkas
Institute of Technology
Hungarian University of Agriculture and Life Sciences,
Gödöllő, Hungary

Supervisor: Prof. Dr. Gábor Kalácska
Institute of Technology
Hungarian University of Agriculture and Life Sciences,
Gödöllő, Hungary

…………………………
Affirmation of supervisor

…………………………
Affirmation of head of school

CONTENTS

LIST OF SYMBOLS, ABBREVIATIONS 5
1. INTRODUCTION, OBJECTIVES 6
1.1. Introduction 6
1.2. Objectives 6
2. MATERIALS AND METHODS 7
2.1. Materials and preparations 7
2.2. Test systems 7
2.2.1. Abrasive pin-on-plate test system 7
2.2.2. Slurry pot test system 8
2.3. Topography.. 8
2.4. Dimensionless numbers 8
2.5. Statistical analysis 8
3. RESULTS 9
3.1. Pin-on-plate system 9
3.1.1. Comparing the materials for wear 9
3.1.2. Comparing the materials for friction temperature evolution 10
3.1.3. Abrasive wear against dimensionless parameters of mechanical properties 11
3.1.4. Multiple linear regression analysis 13
3.1.5. 3D microscopy results and regression models 13
3.1.6. Abrasive sensitivity of the tested materials with the pin-on-plate system 13
3.2. Slurry-pot system 14
3.2.1. Evaluation of the relative wear 14
3.2.2. The daily relative wear 15
3.2.3. The statistical analysis of the wear results 15
3.2.4. 3D surface microscopy results 15
4. NEW SCIENTIFIC RESULTS 16
5. CONCLUSIONS AND SUGGESTIONS 18
6. SUMMARY 19
7. MOST IMPORTANT PUBLICATIONS RELATED TO THE THESIS...20

LIST OF SYMBOLS, ABBREVIATIONS

E	Young's modulus, MPa
F_f	friction force, N
H	Hardness
pv	contact pressure x sliding speed, MPa ms^{-1}
s	Sliding distance, m
S_a	3D surface roughness parameter indicates to Arithmetical mean height, μm
S_{ku}	3D surface roughness parameter indicates to Kurtosis
S_p	3D surface roughness parameter indicates to Maximum peak height, μm
S_q	3D surface roughness parameter indicates to Root mean square height, μm
S_{sk}	3D surface roughness parameter indicates to Skewness
S_v	3D surface roughness parameter indicates to Maximum pit height, μm
S_z	3D surface roughness parameter indicates to Maximum height, μm
σ_F	Flexural strength, MPa
σ_y	Yield stress, MPa
σ_F	Flexural strength, MPa
σ_M	Tensile strength, MPa
σ_C	Compressive strength 1%, MPa
PA66GF30	Polyamide 66 glass fibre reinforced composite
PA6E	Extruded polyamide 6
PA6G	Cast polyamide 6
PA6GESD	antistatic cast polyamide 6 composite
PLA-HF	Biodegradable polymer composite - hemp fibre reinforced polylactic acid
UHMW-PE HD1000	Ultra High Molecular Weight Polyethylene High Density 1000

1. INTRODUCTION, OBJECTIVES

1.1. Introduction

A significant proportion of agricultural machinery is subject to abrasive wear, either in the field of crop production or in animal husbandry machinery. Every year, significant damage is caused by the need to provide spare parts instead of worn machine parts, there is downtime at the machines, and a technological process stops unexpectedly. Machine repairs and maintenance must be provided, and machines must often be equipped with lubrication technology. The abrasive wear is a phenomenon in agricultural machinery that is present in the machine components or even in the complete equipment due to the operating conditions.

In my research, I investigate this issue and use laboratory abrasion tribological modelling to find the relationship between abrasive resistance and material properties for conventional and bio-polymeric materials in systems modelling different abrasion mechanisms.

1.2. Objectives

Development of laboratory models of two dominant abrasion effects (cutting, micro-cutting and abrasive erosion) typical of agricultural machinery according to DIN50322 wear test standard. Design of abrasive pin-on-plate and slurry-pot systems, conversion of the existing tribotesters to the planned abrasion tests.

In the developed two test systems abrasive tribotesting with the following materials. Among the polymers used for abrasion in general engineering practice are PA6G, PA6E, PA66GF30, PA6GESD and UHMW-PE HD1000 are selected. Furthermore, a fully biodegradable polymer composite PLA-HF is involved into the tests.

Comparison of wear test results, evaluation of a large number of measurement data by multiple linear regression. Processing of wear test results as a function of material properties $(H, E, \sigma_y, \sigma_c, \varepsilon_B, \sigma_F, \sigma_M)$, and the dimensionless numbers formed from them.

Based on the coefficients of multiple linear regression, to define the “abrasion sensitivity” for each tested material, to determine the material properties and the dimensionless parameters formed from them dominant in terms of abrasive resistance.

In the light of dimensionless parameters exploring the similarity between the two test systems (abrasive pin-on-plate and slurry-pot) based on the independent variables describing the abrasion sensitivity obtained.

To answer the hypothetical question: can a realistic abrasive operating condition be determined where the PLA / HF bio-composite is not inferior in terms of wear resistance than the engineering polymers currently used.

2. MATERIALS AND METHODS

In this chapter, I present the procedures and experimental methods used to achieve my research goals.

2.1. Materials and preparations

Five types of engineering polymers and composites were recommended for investigation, and they are PA6E, PA6G, PA6G-ESD, PA66GF30, UHMW-PE HD1000 and one kind of bio-composite materials PLA-HF.

2.2. Test systems

2.2.1. Abrasive pin-on-plate test system

The cylindrical polymer pin with a given normal load (N) slides (m/s) on the abrasive belt moving underneath. Meanwhile, the attached strain gauges measure the abrasion friction force (N), a sensor records the vertical displacement of the clamping head as wear (mm), and the thermocouple measures the temperature change (°C) in the polymer pin (Fig. 1).

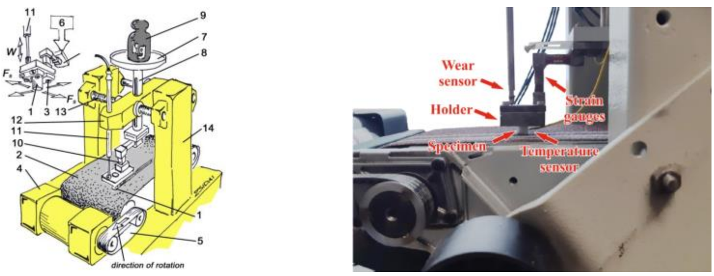

Fig. 1. Schematic figure and a photo about the abrasive pin-on-plate test system

The sampling rate was 5 (1/s). Testing time was set for 10 minutes as the base for the preliminary measurements. The following variables were applied:

- Two types of wear interfaces: P60 and P150 standard abrasive clothes.
- Two sliding speeds: 0.031 m/s and 0.056 m/s
- Three normal loads: 9.81 N, 29.43 N and 49.05 N

With these parameters there are 12 experimental cases.

Table 1. Test cases for the abrasive pin-on-plate test device.

	Test System No.	1	2	3	4	5	6	7	8	9	10	11	12
Test conditions	Load, F_N (N)	9.81	29.43	49.05	9.81	29.43	49.05	9.81	29.43	49.05	9.81	29.43	49.05
	v (m/s)	0.031	0.031	0.031	0.056	0.056	0.056	0.031	0.031	0.031	0.056	0.056	0.056
	Abrasive interface	P60	P60	P60	P60	P60	P60	P150	P150	P150	P150	P150	P150
	Calculated p.v (MPa·m/s)	0.0062	0.0185	0.0308	0.0109	0.0327	0.0544	0.0062	0.0185	0.0308	0.0109	0.0327	0.0544

For the abrasive pin-on-plate test system, polymer specimens were machined into cylindrical pins with an 8mm diameter and a 20 mm length.

2.2.2. Slurry pot test system

Fig. 2 shows the structure of the applied slurry-pot system.

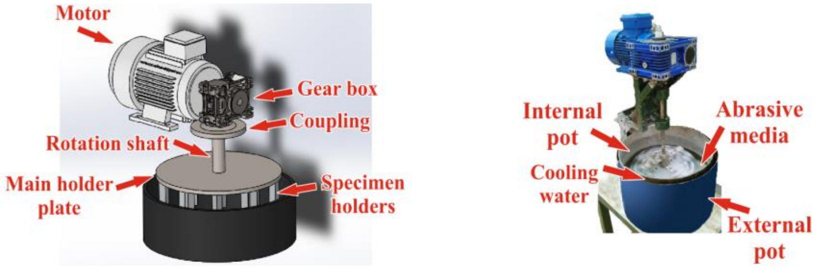

Fig. 2. Assembly of the slurry-pot test system

The electric motor drives a vertical shaft via a worm gear (1:10) and a clutch. The main holder steel plate is fixed to the shaft. Twelve steel columns holding the polymer specimens, arranged on two radii (r_1 and r_2). For this test, the following variables were applied:

- Two speeds: 2.038$m.s^{-1}$ and 1.456 $m.s^{-1}$
- Two types of collisions for the abrasive mediums (tangential and direct)
- Four abrasive mediums.

Four abrasive media were selected for making slurry which are corundum (Al_2O_3) as a reference, gravelly skeletal soil (gravel), lime coated chernozem (loamy soil) and humic sand soil (Sandy soil).

2.3. Topography

For both test systems the 3D polymer surface topography was evaluated before and after a given test. Several parameters were measured based on ISO 25178 (Sq, Ssk, Sku, Sp, Sv, Sz and Sa). using a 3D optical profilometer Coherence Correlation Interferometry (CCI) HD type (Taylor Hobson).

2.4. Dimensionless numbers

All the measured data was evaluated from the function of mechanical properties and from the dimensionless numbers formed from them. The combined dimensionless numbers are: $\frac{H}{E}, \frac{\sigma_y E}{\sigma_M H}, \frac{\sigma_y H}{\sigma_M E}, \frac{\sigma_F \sigma_y}{\sigma_M H}, \frac{E}{\sigma_C}, \frac{\sigma_F}{\sigma_C}, \frac{H\varepsilon_B}{\sigma_y}, \frac{\sigma_C \varepsilon_B}{\sigma_M}, \frac{\sigma_y}{\sigma_C \varepsilon_B}, \frac{\sigma_F H}{\sigma_M E}$

2.5. Statistical analysis

Multiple linear regression models were developed using IBM SPSS 25 software. To examine how a dependent variable depends on several independent variables which are all measured on scales, the main tool is multiple regression.

$$Y = a_0 + a_1 X_1 + a_2 X_2 + \cdots + a_n X_n, \quad (1)$$

If the p-value is less than 0.05, that is, it is significant, then the model is relevant, otherwise it is not.

3. RESULTS

This chapter presents the results that were achieved and discusses them in regard to the scientific findings established.

3.1. Pin-on-plate system

3.1.1. Comparing the materials for wear

Concerning the large on-line registered database, the extremes of test conditions (maximum and minimum loads and speeds) on two types of abrasive clothes. Fig. 3 shows the P60 results: wear in the function of sliding distance with linear approach.

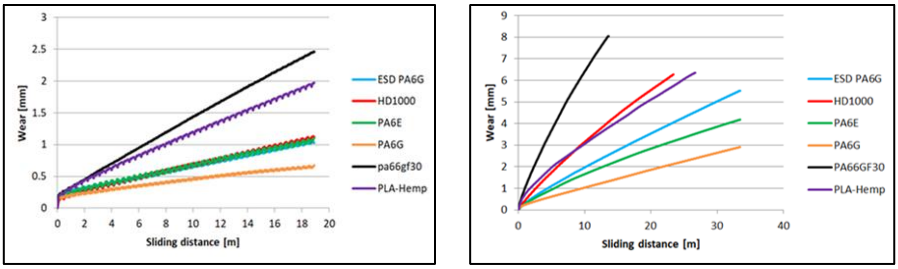

(a) (b)

Fig. 3. The relation between the wear and sliding distance for several polymer types on P60 abrasive clothing. (a) lowest applied pv, (b) highest applied pv

Fig. 3 a) refers to No.1 test condition. PA6G performed the best while PA66GF30 the worst. While for test No. 6, PA6G offered the best wear resistance.

Fig. 4 shows the P150 results: wear in the function of sliding distance.

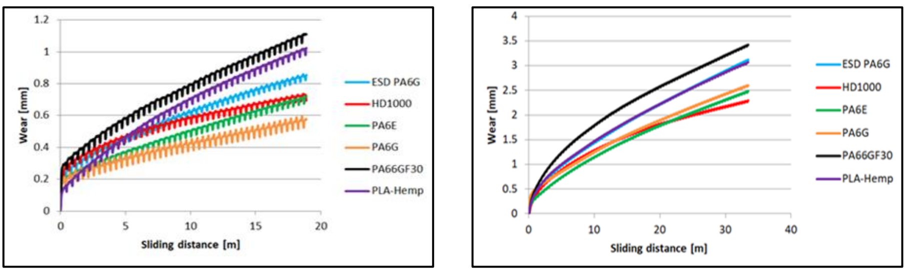

(a) (b)

Fig. 4. The relation between the wear and sliding distance for several polymer types on P150 abrasive clothing. a) lowest applied *pv*, b) highest applied *pv*

Fig. 4 a) refers to No.7 test condition. PA6G performed the best while PA66GF30 the worst. While for test No. 12, PA6E , PA6G and UHMW-PE HD1000 offered the best wear resistances in high pv conditions (Fig. 4 b)).

It is clear that PLA-HF bio-composite was not worse than the average of the tested engineering polymers, in this pin-on-plate system, while PA66GF30 had the highest slope values and it was subjected to the highest wear rate.

Based on the vertical wear values (mm), the area of the cross section of the sample with 8 mm as diameter, the applied load on the specimen (N), and the sliding distance (m), the *specific wear* has been calculated for each test as ($mm^3/N.m$).

The first half meter of sliding is critical from the point of specific wear, that dictates the slopes and positions of the wear lines even further (Fig 5).

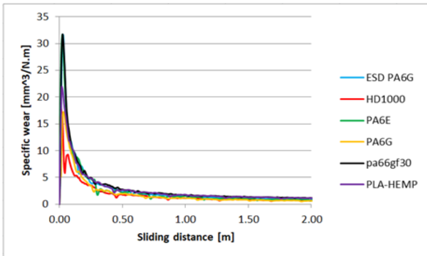

(a)

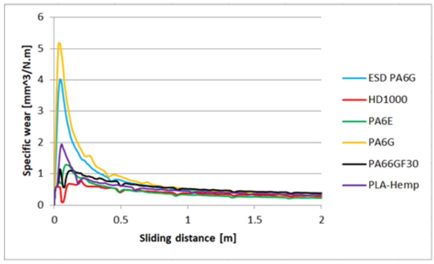

(b)

Fig. 5. The relation between the specific wear and sliding distance for several polymers types. (a) lowest applied pv, (b) highest applied pv (test 1,12)

From Fig. 5, it can also be concluded that the specific wear during running-in for PLA-HF bio-composite was not worse than the average of the tested engineering polymers in this pin-on-plate system. On both P60 and P150 abrasive surfaces, it can be ranked as 4–5th in terms of wear resistance, i.e., similar to UHMW-PE or PA6 ESD, according to the *pv*.

Finally, based on the results, the following can be stated about the wear of polyamides types:

- In all cases PA66GF30 had the highest wear values.
- In all cases PA6G had the lowest wear values.
- In all cases PA6G ESD had the second highest wear values after PA66GF30.
- In all cases PA6E had the second lowest wear values after PA6G.

According to these 4 points, it is clear that the wear order of the polyamide family went, according to the following sequence: PA66GF30 (the highest wear) - PA6G ESD - PA6E - PA6G (the lowest wear).

Parallel with the wear curves, the arising friction force and temperature change in the plastic pin, were recorded on-line too.

3.1.2. Comparing the materials for friction temperature evolution

Similarly to the wear evaluation, the extremes of the test conditions (maximum and minimum loads and speeds, numbered as 1, 12) on two types of abrasive clothes are shown in Fig 6, for the temperature evaluation.

As shown in the Fig. 6, PA6E recorded the highest temperatures, while PA66GF30 the lowest temperature, which can not be explained by the similar thermal properties. However, it is a fact that PA6E has the lowest heat deflection temperature, high specific heat. The resulted temperature evolution a much more complex phenomenon in accordance with Archard's friction theory.

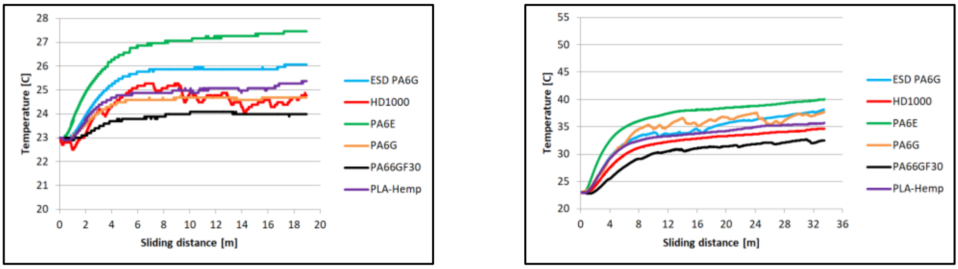

(a) (b)

Fig. 6. The relation between the temperature evolution and sliding distance for several polymer types. (a) lowest applied pv, (b) highest applied pv

As shown in the Fig. 6, PA6E recorded the highest temperatures, while PA66GF30 the lowest temperature, which can not be explained by the similar thermal properties. However, it is a fact that PA6E has the lowest heat deflection temperature, high specific heat. The resulted temperature evolution a much more complex phenomenon in accordance with Archard's friction theory.

3.1.3. Abrasive wear against dimensionless parameters of mechanical properties

Based on the mechanical properties of the materials used, ten dimensionless numbers were derived, which can characterize each polymers. Taken the wear values of on-line wear curves (obtained at the last measurable point in all test systems for all materials). However, the whole project focuses on 6 selected polymers, it is clear that the 4 polyamide types can perform clear trends at this type of evaluation and many new results were thus revealed.

1. Wear evaluation against H/E

The calculated quotients *(hardness / elasticity modulus)* are in Table 2.

Table 2. The H/E values for the materials used

The dimensionless number	**PA6G**	**PA6E**	**PA66GF30**	**UHMW-PE HD1000**	**PA6G ESD**	**PLA-HF**
$\frac{H}{E}$	0.0034	0.0030	0.0023	0.0100	0.0028	0.0004

Focusing on the polyamides in Table 2 the decreasing order of $\frac{H}{E}$ values were as follows (PA6G - PA6E - PA6G ESD - PA66GF30), this order is the exact opposite order of the highest wear values that were shown in 3.1.1. As a result, there is an inverse relation between H/E and the wear. By increasing the values of H/E the wear is increasing.

Fig. 7 shows that the polyamide family performed a decreeing trend as a relation with $\frac{H}{E}$, while both the PLA-HP and UHMW-PE HD1000 were out of this trend. From all dimensionless number figs, it can be concluded that the wear resistance order for polyamides described in 3.1.1 can be well approached with the combined dimensionless numbers, at some cases the UHMW-PE HD1000 and PLA-HF could be involved into the same evaluating trends as written in the following:

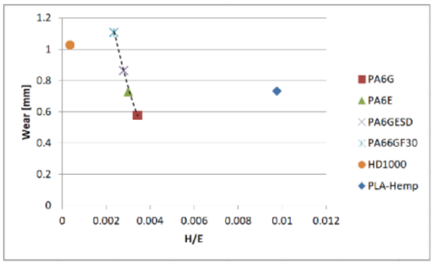

Fig. 7. Typical relation between wear at the last measurable point of test and $\frac{H}{E}$ dimensionless number combined from mechanical properties

Proportional relation

- There are proportional relations between the wear values of all the tested polyamide types (PA66GF30, PA6G ESD, PA6G and PA6E) and $\frac{\sigma_y E}{\sigma_M H}$, as well as $\frac{\sigma_y}{\sigma_C \varepsilon_B}$. By increasing dimensionless number values a higher wear value was measured.
- Also there are proportional relations between the wear values of three polyamides (PA66GF30, PA6G and PA6E) and $\frac{\sigma_F}{\sigma_C}$. The trend is followed by the UHMW-PE HD1000, too.
- $\frac{\sigma_F \sigma_y}{\sigma_M H}$ offers such a proportional relation with wear, where 5 materials follow the trend-line except for UHMW-PE HD100.

Inverse relation

- There are inverse relations between values $\frac{H}{E}$, $\frac{\sigma_y H}{\sigma_M E}$, $\frac{\sigma_F H}{\sigma_M E}$ and the wear of polyamides (PA66GF30, PA6G ESD, PA6G and PA6E). By increasing dimensionless number values a lower wear value was measured.
- There are inverse relations between values $\frac{H \varepsilon_B}{\sigma_y}$ and the wear of three polyamides (PA6G, PA6E and PA6G ESD), the trend was followed by PLA-HF, too. By increasing the dimensionless number value, a lower wear value was measured.
- Calculating $\frac{\sigma_C \varepsilon_B}{\sigma_M}$, loosen inverse relation was found concerning all the tested six polymers.

However, the combined dimensionless numbers analyzed above, were not studied in such details, and even the new findings between wear and combined properties valid for polyamides and UHMW-PE together, have not been published yet.

3.1.4. Multiple linear regression analysis

Large amount of data was evaluated with the statistical models developed. Multiple linear regression models analyzed the impact of material properties and test system characteristics.

Wear, using P60 abrasive: The best fitting model was Eq. 2:

$$\text{wear} = a_0 + a_1\text{s} + a_2\text{F}_N + a_3 \cdot \frac{\sigma_y}{\sigma_c \varepsilon_B} + a_4\text{H} \tag{2}$$

The F-value of the model was $9.619 \cdot 10^4$ and $p < 0.001$, thus this model is relevant. For this model, the goodness-of-fit is $R^2 = 0.831$.

3.1.5. 3D microscopy results and regression models

Concerning the change of the polymer surfaces, white light 3D microscopy Fig. 8 shows the surface 3D topography of the HD1000 before and after testing.

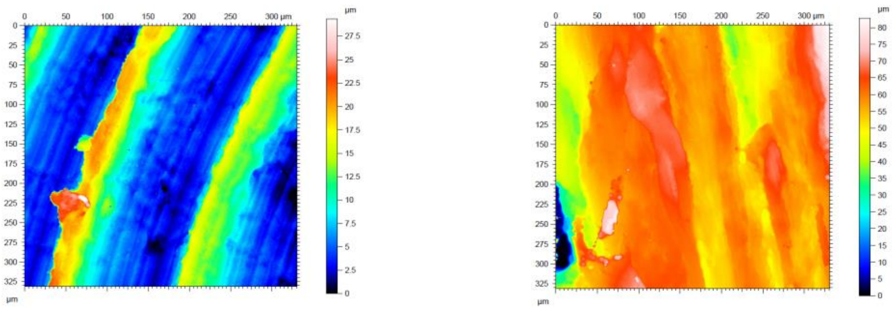

UHMW-PE HD1000 (before) UHMW-PE HD1000 (after)

Fig. 8. Microscopic visualization of the surface 3D topography of HD1000

The 3D surface data were analyzed by multiple linear regression models, too. The dependent variables were the 3D surface parameters, while the independent variables were the sliding distance, load, the calculated *pv*, the sliding velocity, the material properties and the derived dimensionless numbers from them.

Sq, P150: For Sq, the best fitting model among the possible ones is as Eq. 3.

$$Sq = 6.057 + 0.052s - 0.00014E \tag{3}$$

the F-value of the model was 15.989 and $p = 0.001$, thus the model is relevant. For this model the goodness-of-fit is $R^2 = 0.804$, E has the highest effect.

3.1.6. Abrasive sensitivity of the tested materials with the pin-on-plate system

In the final statistical evaluation of the pin-on-plate test results, many novel research results are summarized:

- Introducing the abrasive sensitivity of the tested materials based on the standardized coefficients of multiple regression models,
- Ranking the abrasive sensitivity of the materials according to the independent variables of the test systems.

Consider a dependent variable (e.g. wear, etc.) and those material properties and indicators formed from them which has a significant affect on it. The abrasive sensitivity, is the extent of how the independent variables affect it, which is related to the standardized regression coefficients. The sensitivity can be visualized in 2D map constructed for Table 3 showing the abrasive sensitivity for wear, abrasive friction force, heat generation and the 3D parameters. The factors are in an increasing order of affect.

Table 3. 2D map of abrasive sensitivity in pin-on-plate system

factors in increasing abrasive sensitivity to system variables				
	less dominant		**more dominant**	
Wear, P60	H	$\frac{\sigma_y}{\sigma_c \varepsilon_B}$		
Wear, P150	$\frac{\sigma_y}{\sigma_c \varepsilon_B}$			
F_f, P150	H	$\frac{\sigma_F \sigma_y}{\sigma_M H}$		
ΔT, P60	H	$\frac{H \varepsilon_B}{\sigma_y}$	$\frac{\sigma_F H}{\sigma_M E}$	σ_F
Sq, P150	E			
Ssk, P60	σ_F			

3.2. Slurry-pot system

3.2.1. Evaluation of the relative wear

The relative wear of the different polymer samples - daily cumulative of the weight loss as a percentage (%) compared to the zero day weight – is evaluated for the applied slurry materials. Fig. 9 shows the relative wear according to the four different abrasive medias, position 1.

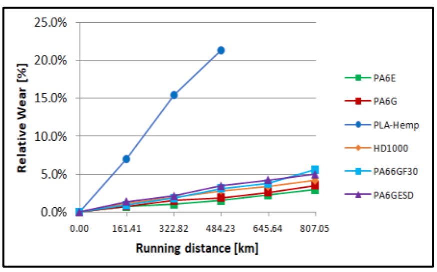

(Corundum)

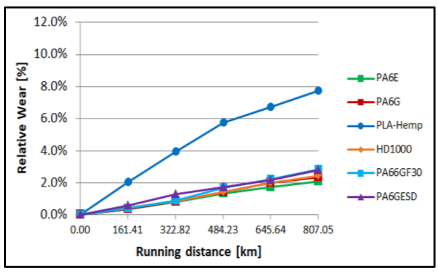

(gravel)

Fig.9. The relative wear of the tested materials

It is clear, that PLA-HF composites were more sensitive for the slurry-pot conditions, than for the pin-on-plate abrasive dry cutting. While on the dry pin-on-plate system the bio-degradable composite had an average wear resistance among the engineered plastics, in the corundum slurry system the PLA-HF suffered a severe material loss and was not comparable with the engineered polymers. For the gravel soil, the PA6E had performed the best wear resistance. With the loamy slurry media, the PA6G was the best. The PA6E suffered the least wear in the sandy system.

3.2.2. The daily relative wear

The daily relative wear of the weight loss as a percentage (%), compared to the previous day's weight was also determined.

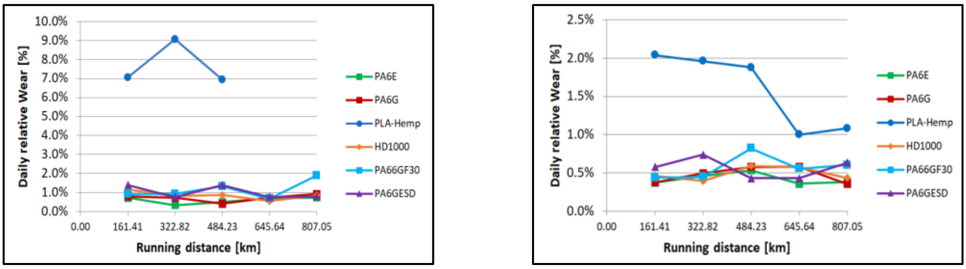

(a) (b)

Fig. 10. Daily relative wear in position 1 with (a) corundum (b) gravel

It is clear, that the PLA-HF had a running-in like effect during the first two to three days, which was caused by the fast wear of the coating layer of the composites.

3.2.3. The statistical analysis of the wear results

Wear, Corundum: The best fitting model is as Eq. 4;

$$\text{wear} = -0.234 + 1.246t - 1.931\,ca + 0.76 \cdot \frac{\sigma_y}{\sigma_c \varepsilon_B} \tag{4}$$

The F-value of the model is 119.6 and $p < 0.001$, thus the model is relevant. For this model the goodness-of-fit is $R^2 = 0.722$.

3.2.4. 3D surface microscopy results

The evaluation of the 3D surface topographic changes were similar to those already presented in the pin-on-plate system. It is clear that by the end of the slurry abrasive erosion, the original machining marks of the surfaces have completely disappeared due to the swirling slurry. For all cases, the results are completely converted surfaces to differing degrees, while PLA-HF - beside the surface change - suffered essential deformation due to the internal stress release.

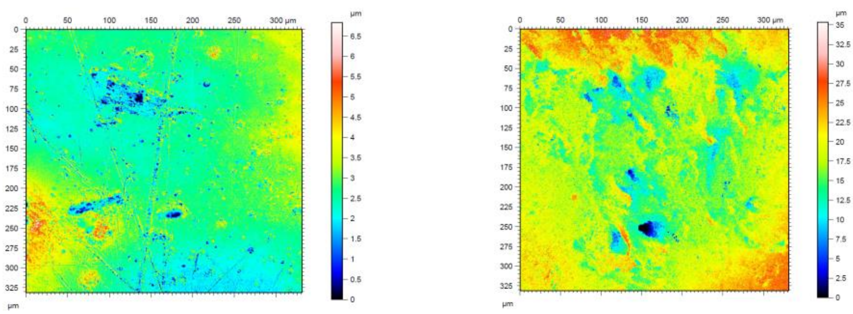

PLA-HF (before) PLA-HF (after)

Fig. 11. The PLA-HF surfaces before and after measurements

4. NEW SCIENTIFIC RESULTS

For the investigated engineering plastics PA6E, PA6G, PA6G-ESD, PA66GF30, UHMW-PE HD1000 and one kind of bio-composite materials PLA-HF, I made the following statements under broad system conditions, in relation to tribological system results and material properties and the dimensionless characteristic numbers formed from them.

1. Abrasive wear in pin-on-plate

Concerning the tested materials I found that there is proportional relation between wear and dimensionless numbers, in different areas of validity. Wear of polyamides (PA66GF30, PA6G ESD, PA6G and PA6E) all correlated with $\frac{\sigma_y E}{\sigma_M H}$, and $\frac{\sigma_y}{\sigma_C \varepsilon_B}$. All engineering plastics (polyamides and UHMW-PE HD 1000) correlated with $\frac{E}{\sigma_C}$, furthermore polyamides and bio-composites with $\frac{\sigma_F \sigma_y}{\sigma_M H}$. There was no dimensionless parameter proportional to the wear of all engineering plastics and bio-composites.

I found that the areas of validity of the inverse proportionality between wear and dimensionless numbers differ from the validity of direct proportionality. Wear of polyamides (PA66GF30, PA6G ESD, PA6G and PA6E) correlated with $\frac{H}{E}$, $\frac{\sigma_y H}{\sigma_M E}$, $\frac{\sigma_F H}{\sigma_M E}$ and three polyamides (PA6G, PA6E and PA6G ESD) and the bio-composite (PLA-HF) with $\frac{H \varepsilon_B}{\sigma_y}$. Calculating $\frac{\sigma_C \varepsilon_B}{\sigma_M}$, loosen inverse relation was found concerning all the tested six polymers.

2. Abrasive friction force in pin-on-plate

I found that the abrasive friction resistance of the PLA-HF material is 80-90% higher compared to the five engineering polymers tested. I proved by microscopic images that the main reason for this is the continuous tearing and shearing of the HF fibres on the surface of the PLA-HF during sliding.

3. 3D surface topography in pin-on-plate and slurry systems

I concluded that in parallel with the abrasive wear process, the transformation of the surface geometry is bi-directional. I proved with 3D surface topography analyses that in the case of the tough, highly deformable UHMW-PE HD1000 and PA6E, the deformations occur in a larger material cross-section, the micro-geometric parameters (Sp, Sv, Sz, Sa) increased beside decreased Skewness (Ssk) -meaning that the asperities, the surface material is elevated and deformed above the mean plane – and increased Kurtosis (Sku) meaning that the height distribution is more spiked due to the cutting effect. On the contrary, the more rigid PA66GF30 due to the cutting effects performed increased Skewness – the height distribution is skewed below the mean plane in accordance with the experienced wear values – and decreased Kurtosis (Sku) resulting more indented portion on the surface.

4. Abrasive sensitivity as system approach method for both test systems

I introduced the abrasive sensitivity analyses as a system approach method. The abrasive sensitivity is the extent of how the independent variables - the sliding distance "s", the load "F_N", the sliding velocity "v", the material properties and the dimensionless numbers formed from them - affect the tribo results (wear, friction force, heat generation and change of 3D topography), which is related to the standardized regression coefficients of the models developed. The higher the absolute value of the corresponding standardized regression coefficient is, the higher the abrasive sensitivity of the dependent variable (wear, friction, temperature, surface 3D properties). I worked out such a 2D map visualization of the abrasive sensitivity, where the rank of all impacting factors on the all examined dependent variables are highlighted.

5. The change of the polymers' 3D surface characteristics

By means of IBM SPSS 25 software I developed multiple linear regression models and stated for the slurry test systems that wear and the change of the polymers' 3D surface characteristics are sensitive mainly for the tensile features e.g. $\frac{\sigma_y E}{\sigma_M H,}$, E and ε_B, while the compressive and flexural properties, unlike the pin-on-plate system, played a lesser role. I concluded that some parameters appear in both test system's sensitivity analyses. Wear with P60, P150 pin-on-plate and with gravelly skeletal soil slurry, the $\frac{\sigma_y}{\sigma_C \varepsilon_B}$ is important among the material characteristics. The appearance of the compressive strength is in accordance with the mode of the complex load of micro-geometries. In both test systems, E is important for the change of 3D surface parameters. This reflects on the role of deformation capability of the surface micro-geometry.

5. CONCLUSIONS AND SUGGESTIONS

Abrasive pin-on-plate and slurry-pot systems were applied to study the abrasive behaviour of five engineered polymers and a bio degradable composite. The measured friction, wear and heat generation and 3D surface change, were analysed in conventional ways (graphs, microscopic photos), and furthermore, by means of multiple linear regression models, developed using IBM SPSS 25 software. Concerning the tested materials, the "sensitivity to abrasion" was introduced, based on the multiple linear regression models, taking the standardized beta regression coefficients into account.

In abrasive pin-on-plate systems (on P60 and P150 particles), where the cutting effect is dominant:

PA6G offered the best abrasive resistance while PA66GF30 the worst. The bio-polymer (PLA-HF) was average among the engineered polymers. There are proportional relations between the wear values of the polyamides and $\frac{\sigma_y E}{\sigma_M H}$, as well as $\frac{\sigma_y}{\sigma_C \varepsilon_B}$. A similar trend is valid for the polyamides and UHMW-PE HD1000 in the case of $\frac{E}{\sigma_C}$.

There are reciprocal relations between values $\frac{H}{E}, \frac{\sigma_F H}{\sigma_M E}$ and the wear of polyamides (PA66GF30, PA6G ESD, PA6G and PA6E).

$\frac{\sigma_F \sigma_y}{\sigma_M H}$ offers such a proportional relation with wear, that 5 materials follow the trend-line except UHMW-PE HD1000.

In slurry-pot systems:

PLA-HF had the worst abrasive resistance, while the engineered polymers offered similar wear trends, the PAE and PA6G being the best ones.

Concerning the wear speed on a daily base, the PLA-HF had a running-in like effect during the first period of testing.

Sensitivity analyses proved that the varying abrasive load conditions bring different material characteristic groups (e.g. tensile, compressive, flexural) to the fore. Some parameters appear in other system conditions:

Wear P60, P150 and gravel: $\frac{\sigma_y}{\sigma_C \varepsilon_B}$ is important among the material characteristics.

In slurry-pot and pin-on-plate, E is important for the change of 3D surface parameters.

As a follow up to this research, further investigations and activities may be required. I suggest to improve the performance of the bio-composite materials by using a high wear resistant coating layer, testing several types of bio-composite materials and initiate real field trials of these used materials and see how other parameters could affect the wear performance like the dynamic load, changing ambient temperature and humidity.

6. SUMMARY

To summarize, two different test systems were designed to evaluate the tribological behavior of 5 engineering plastics (PA6E, PA6G, PA66GF30, PA6GESD and UHMW-PE HD1000) and a fully degradable bio-composite (PLA-hemp fiber), targeted for agricultural machinery's abrasive conditions.

For both test systems, the 3D polymer surface topography was evaluated before and after a given test by using a Taylor-Hobson white light microscope.

All the results and the 3D parameters' values were evaluated and analyzed statistically using IBM SPSS 25 software by developing multiple linear regression models. To examine how a dependent variable depends on several independent (or explanatory) variables, which are all measured on scales, the primary instrument is multiple regression. This tool is also used to examine the sensitivity of the material properties and the test system characteristics, on tribological behavior.

The results of the pin-on-plate test system show that PA6G offered the best abrasive resistance while PA66GF30 the worst. The PLA-HF was average among the engineering polymers. Multiple regression models proved that the tribo results showed high sensitivity and relation with σ_F, σ_C, both alone and in derived dimensionless forms. The change in the surface 3D parameters correlated mainly with E and σ_F, σ_C.

For the slurry-pot system, the results show that PLA-HF had the worst abrasive resistance, while the PA6E and PA6G were the best ones. Concerning the wear speed on a daily base, the PLA-HF had a running-in like effect during the first period of testing, caused by the fast wear of the coating layer of the composites. The engineering polymers including the composite PA66GF30 and PA6G ESD showed less fluctuation in daily wear than the PLA-HF.

Based on the coefficients of the regression models, I developed and introduced the "abrasion sensitivity" maps. In the slurry-pot system, the sensitivity analyses enhanced the primary role of tensile features e.g. $\frac{\sigma_y E}{\sigma_M H,}$, E and ε_B, while the compressive and flexural properties, unlike the pin-on-plate, played a lesser role.

Sensitivity analyses proved that the varying abrasive load conditions bring different material characteristic groups into account. Some of these parameters appeared in both system conditions like $\frac{\sigma_y}{\sigma_C \varepsilon_B}$. Also E has been considered as an important factor for the change of the 3D surface parameters. This reflects on the role of the deformation capability of the surface micro-geometry.

7. MOST IMPORTANT PUBLICATIONS RELATED TO THE THESIS

Refereed papers in foreign languages:

1. **Muhandes**, **H.**, Kalacska, G., Kadi, N., Skrifvars, M. (2017): Thermoplastic bio-composite based on cellulose fibers, V. Synergy International Conference, Engineering, Agriculture and Green Industry Innovation, Mechanical Engineering Letters, Vol. 15, pp. 7-15.
2. Kalacska, A., **Muhandes**, H., (2018): 3D topographical analysis of abrasive worn surfaces, Mechanical Engineering Letters, Vol. 17, pp. 47-56.
3. **Muhandes**, H., Kalacska, G., (2019): A slurry-pot abrasive wear test device for several composite materials, International Journal of Engineering and Management Sciences, Vol. 4, No. 1, pp. 437-444, doi: 10.21791/IJEMS.2019.1.54.
4. **Muhandes**, H., Kalacska, A., Kalacska, G. (2020): Analyses of abrasive wear behaviour in pin-on-plate tribo-system for several materials, IOP Conf. Series: Materials Science and Engineering 749 (2020) IOP Publishing, doi:10.1088/1757-899X/749/1/012020.
5. **Muhandes**, H., Kalacska, A., Székely, L., Keresztes, R., Kalacska, G. (2020): Abrasive sensitivity of engineering polymers and a bio-composite under different abrasive conditions. Materials 13(22): 5239. (IF: 3.057)
6. **Muhandes**, H., Kalacska, G. (2020): Bio-degradable Polymer composites as abrasive wear materials. Polymer Sci Peer Rev J. 1(3). PSPRJ. 000512.

Refereed papers in Hungarian:

7. **Muhandes**, H., Kalacska, G. (2018): Kompozit anyagok abrazív koptató vizsgálata pin-on-plate tribométerrel, Műanyagipari Szemle, 06. szam, 1-10. ISSN 1785-7856.
8. **Muhandes**, H., Kalacska, G. (2020): Mezőgazdasági gépek polimer alapanyagainak abráziós kopásállósága “slurry-pot” mérések alapján, Műanyagipari Szemle (accepted).